JOURNAL OF CATALYSIS **104**, 186–201 (1987)

Investigation of the SO_2 Oxidation Rate Limiting Factors for K/V and Cs/V Catalysts at Low Temperatures

F. J. DOERING, H. K. YUEN, P. A. BERGER, AND M. L. UNLAND

Monsanto Chemical Company, 260 Springside Drive, Akron, Ohio 44313

Received July 1, 1986; revised October 14, 1986

Different potassium and cesium vanadyl sulfate catalysts were studied to determine why cesium produces a more active catalyst at low temperatures than potassium. Thermal analyses and electron paramagnetic resonance instruments were used to study catalysts in various SO_2–SO_3–O_2–N_2 atmospheres at normal operating temperatures. Catalysts supported on controlled pore glass silica were analyzed. The results indicate that K/V catalysts form large amounts of inactive V^{4+} crystals at temperatures under 425°C while the Cs/V catalysts form much smaller amounts at temperatures below 400°C. The reaction rates at temperatures below 425°C drop off because a K_2SO_4–V_2O_4–SO_3 compound crystallizes out of the active molten salt in the K/V catalyst. The Cs/V catalyst activity is believed to drop off below 400°C because increased V_2O_4–SO_3 concentrations reduce the availability of V_2O_5 for SO_2 oxidation according to the six-step Boreskov reaction mechanism.

INTRODUCTION

Many reaction mechanisms and kinetic equations have been proposed for the oxidation of SO_2 to SO_3 with vanadium catalysts (*1–4*). Because of improved analytical instruments in recent years, much has been published (*2–4*) on physical measurements of the catalyst, a molten salt of V_2O_5 in potassium pyrosulfate dispersed on a silica support. Electron paramagnetic resonance (EPR) spectroscopy has been used for evaluating the V^{4+} ion in the catalyst during reaction conditions (*5–10*). Grydgaard *et al.* (*5*) plotted data from others' EPR measurements (*6–8*) and found that the function

$$K = \frac{(V^{4+})^2}{(V^{5+})^2 p_{SO_2}} \tag{1}$$

gave a straight line when ln K vs $1/T$ was plotted. This function held well for catalysts that were equilibrated with the reaction gas or that had thin liquid films on the catalyst surface. It was shown, however, that as the film thickness increased, V^{4+} content went up. Grydgaard *et al.* (*5*) then proposed the following mechanism:

$$2X + SO_2 \rightleftharpoons 2Y \tag{2}$$

$$2Y \rightleftharpoons 2Z + SO_3 \tag{3}$$

$$2Z + \tfrac{1}{2}O_2 \rightleftharpoons 2X \tag{4}$$

where X is a V^{5+} species and Y and Z are V^{4+} species. Reaction (3) was assumed to be far from equilibrium in thin films and in equilibrium in thick films. Thick films would give Mars and Maessen's (*9*) model (joining reactions (2) and (3)) and thin films would give Boreskov's (*8*) model (joining reactions (3) and (4)). When V^{4+} precipitation was assumed in the kinetic model, the break in the Arrhenius plots disappeared.

Boreskov *et al.* (*6*) ran a commercial catalyst in 95% preconverted gas on EPR. A hyperfine structure at high temperatures was attributed to VO^{2+} ions. A single assymetrical line appeared below 470°C and it was inferred that a V^{4+} solid phase was separating from the melt. A catalyst reduced in 30% preconverted gas at 400°C produced a sharp single line on the EPR spectrum and had parameters close to those of a $VOSO_4$ spectrum. Mastikhin *et al.* (*7*) performed EPR measurements on catalysts with different film thicknesses. The degree of vana-

0021-9517/87 $3.00

dium reduction was shown to rise with an increase in film thickness. The film surface layer was believed to be oxidized to a greater degree than the deep layers due to different diffusion rates of SO_2 and O_2. At the break on the Arrhenius curves where the reaction's activation energy suddenly increased, the V^{4+} content apparently exceeded its solubility limit, and a V^{4+} compound began to precipitate from the melt. Catalysts with thin films of molten salt had Arrhenius breaks 110°C lower than the industrial catalysts. Boreskov *et al.* (*8*) studied a bidisperse silica gel catalyst with a high surface area, 6.5% V_2O_5, $K/V = 3.5$. The oxygen content of the gas was either 0.36 or 7.8% and steady state results on EPR gave the same degree of vanadium reduction over the temperature range 360–500°C. Replacing the reaction gas with argon or 5% O_2/N_2 oxidized the catalyst at the same rate. Thus, oxygen diffusion did not affect the V^{4+} content. The oxidation of V^{4+} in the catalyst was believed to take place at the expense of SO_3 which was bound to the active component. The vanadium oxidation and reduction rates were shown to be first order which indicated dinuclear complexes of vanadium compounds. Ponomarev *et al.* (*10*) studied a $K/V = 3$ molten salt at low conversions with EPR. Non-steady state conditions for the catalyst were made by continuous admission of the molten salt with a fixed composition into a reactor at various temperatures and oxygen concentrations. The activation energies for step 1 in the forward and reverse directions and for step 2 of the two-step Mars and Maessen mechanism (*9*) were calculated from the data. The rate-limiting step was oxidation of V^{4+} with an activation energy of 21.1 kcal/mol (88.2 kJ/mol), and an inactive V^{4+} phase had to be accounted for as temperature was decreased.

Other analytical methods were used to gain more insight on the reaction chemistry. Holroyd and Kenney (*11*, *12*) looked at the unsupported $K_2S_2O_7$–V_2O_5 molten salt in unconverted SO_2 gas. Absorption rates of SO_2 and O_2 in well-stirred melts between 360 and 480°C were measured. The absorption rates for SO_2 and O_2 were much faster than the overall reaction rate. Holroyd (*11*) found that a V^{4+} precipitate formed in the molten salt, and any concentrations of V^{4+} greater than 4% mole fraction at 440°C were insoluble. Ezhkova *et al.* (*13*) did XRD and IR work on the $VOSO_4$–K_2SO_4 system. A comparison of IR spectra of $VOSO_4$ and K_2SO_4 with those of mixtures showed that the mixtures formed vanadium complexes in which the sulfate groups were strongly coordinated to the vanadyl group. Hahle and Meisel (*14*) used X-ray and differential thermal analysis (DTA) methods on the vanadium molten salts. The $K/V = 2.5$ molten salt was found to melt in the range 340–350°C, and above 370°C a homogeneous melt was obtained. By reducing mixtures with H_2S, the principal melting range for the molten salt increased to 380–450°C. Wolf *et al.* (*15*) obtained the $K/V = 3$ molten salt melting properties, vanadium reduction data, and SO_3 contents in various gases. SO_2 gas reduced the V^{5+} to V^{4+} and a crystalline phase was detected by X ray. O_2 oxidized V^{4+} to V^{5+} and formed a glass. SO_3 absorbed into the melt and some crystal was detected by X ray. The work (*15*) concluded that the V^{4+} crystal increased the melting points of the salts when exposed to the following gases: 280–310°C in O_2, 348°C in SO_3, 400°C in N_2, 470–500°C in SO_2–O_2–N_2 gases, and 540°C in SO_2. Guo *et al.* (*16*) studied K/V and K/Na/V catalysts by XRD, SEM, and thermal analyses. A two-step reaction mechanism with two vanadium complexes explained their data well when V^{4+} precipitation was taken into account.

The transient response (relaxation) method for evaluating the SO_2 oxidation catalyst has contributed important insight for the reaction mechanism. Boreskov *et al.* (*17*) proposed a six-step mechanism after varying SO_2 and O_2 concentrations over a $K/V = 3.5$ gradientless catalyst bed and analyzing SO_2 and O_2 in a 30 second chromatograph:

$$V_2O_5 + SO_2 \rightleftharpoons V_2O_5\text{–}SO_2 \quad (5)$$

$$V_2O_5\text{–}SO_2 + \tfrac{1}{2}O_2 \rightleftharpoons V_2O_5\text{–}SO_3 \quad (6)$$

$$V_2O_5\text{–}SO_3 \rightleftharpoons V_2O_5 + SO_3 \quad (7)$$

$$V_2O_5\text{–}SO_2 \rightleftharpoons V_2O_4\text{–}SO_3 \quad (8)$$

$$V_2O_4\text{–}SO_3 \rightleftharpoons V_2O_4 + SO_3 \quad (9)$$

$$V_2O_4 + \tfrac{1}{2}O_2 \rightleftharpoons V_2O_5. \quad (10)$$

Steps 6 and 10 were said to be rate determining and first order with respect to oxygen. Combining steps 5 and 8 through 10 will give reaction mechanisms (2) to (4). Kozyrev *et al.* (*18*) dropped temperature rapidly from 485 to 420°C while flowing preconverted 4% SO_2, 10% O_2 gas over a K/V = 3 catalyst and analyzing with both EPR and the chromatograph of (*17*). The dissolved V^{4+} ions immediately increased by a factor of 1.5 to 2 and then did not change. The inactive V^{4+} phase grew very slowly along with SO_2 gas content. A sudden increase in the temperature led to a rapid restoration of the catalyst. The initial rapid reduction of V^{5+} was due to reaction (8) moving to the right. The inactive V^{4+} phase formed very slowly due to precipitation which quickly reversed when temperature was increased. The V^{4+} ions in the melt were assumed to be directly involved in reaction catalysis.

Chumachenko *et al.* (*19*) determined rate constants and activation energies for the individual steps of the proposed six-step reaction mechanism (*17*). The transient response method evaluated the effect of hitting oxidized or reduced catalyst with SO_2/O_2 gases. The rate of interaction of V^{4+} with SO_3 was found to be much higher than the V^{4+} oxidation with O_2. A delay in SO_3 evolution on the reduced catalyst was assumed to be caused by slow dissolution of the crystalline V^{4+} in the melt.

Balzhinimaev *et al.* (*20*) used a mass spectrometer to evaluate transient response of various feed streams on a K/V = 5 molten salt. Their results indicated that two reaction mechanisms were possible: associative, without changes in the vanadium valence state (5–7), or reduction/oxidation (steps 5, 8–10). Formation of a peroxide due to the interaction of two electrons of a dinuclear V^{4+} complex with a vacant orbital of O_2 was predicted. This was supported by the fact that oxidation of completely reduced samples required one molecule of O_2 for two atoms of V^{4+}. With a decrease in temperature, step 8 would be expected to move to the right because of preferred intramolecular oxidation of the $V_2O_5\text{–}SO_2$ (sulfite) complex to a $V_2O_4\text{–}SO_3$ (sulfate). Lower temperatures also would produce the availability of more SO_3 to reduce the concentration of sulfite complexes which would be required for molecular oxygen addition in step 6. The net result would be formation of V^{4+} compounds precipitating from the melt. Later work (*21*) obtained diffusion and solubility coefficients of O_2, SO_2, and SO_3, and indicated that the dinuclear vanadium complex coordinates several pyrosulfate ligands. Results of dissolution showed that SO_2 tends to form various associates with charged particles in the melt.

Detailed investigations (*22–24*) on vanadium chemistry in the molten salt gave further evidence that the mechanistic suggestions of (*20*) could occur. Hansen *et al.* (*22*) did potentiometric, cryoscopic and spectrophotometric work on the $K_2S_2O_7\text{–}K_2SO_4\text{–}V_2O_5$ system and suggested that the equilibrium

$$VO(SO_4)_3^{-3} + SO_4^{-2} \rightleftharpoons VO_2(SO_4)_2^{-3} + S_2O_7^{-2} \quad (11)$$

where only $VO_2(SO_4)_2^{-3}$ is catalytically active, can explain the V^{5+} chemistry. Krasil'nikov *et al.* (*23*) used X-ray diffraction, optical immersion control, infrared spectroscopy, and EPR on the $K_2O\text{–}V_2O_4\text{–}SO_3$ system and found $K_2(VO(SO_4)_2)$ and $K_2(V_2O_2(SO_4)_3)$ to be the main V^{4+} compounds. Oxidation of these compounds in air gave

V^{5+} compounds similar to Hansen's (*22*). Mastikhin *et al.* (*24*) used NMR on K/V melts and catalysts under reaction conditions to show that vanadium is coordinated to pyrosulfate ions which rapidly exchange with the molten pyrosulfate.

Thus, much progress has been made in recent years on the understanding of the chemistry of the K/V catalysts during SO_2 oxidation. Many researchers have shown that V^{4+} precipitation from the molten salt is the cause for the break in the Arrhenius plots at low temperatures. Some of the most significant findings in the literature are the following:

(1) When V^{4+} precipitation was assumed in a kinetic model, the break in the Arrhenius plots disappeared (*5*, *8*).

(2) EPR data showed that the degree of vanadium reduction rose with an increase in molten salt film thickness (*7*). Thin films of molten salt gave the same degree of vanadium reduction irregardless of gaseous oxygen content (*8*).

(3) Transient response data (*17–20*) indicated that two reaction mechanisms were possible. An associative mechanism without changes in the vanadium valence state was based on preferred intramolecular oxidation of a V_2O_5–SO_2 complex to a V_2O_4–SO_3 complex at lower temperatures.

To provide more data on the reaction chemistry, we studied the K/V and Cs/V catalysts under reaction conditions on a Mettler thermal analyzer and on an EPR spectrometer. By comparing the two different types of catalysts, we hoped to gain more insight on the reaction chemistry.

EXPERIMENTAL METHODS

The EPR and thermal analyses were done on controlled pore glass (CPG) catalysts similar to those used for kinetic studies (*25*). The CPG support had an average pore diameter of 2574 Å, 14.3 M^2/g surface area, and 1.44 cm^3/g pore volume. An SO_2 generator was built so that a premixed gas, usually 10% SO_2, 11% O_2, and 79% N_2, could be preconverted up to 95% and then sent to the thermal analyzer or EPR spectrometer. The flow diagram for the SO_3 generator is in Fig. 1. 10 g of 8–20-mesh commercial vanadium catalyst were used in the reactor to convert about 100 scc/min (standard cubic centimeters at 1 atm and 0°C) of the feed gas to 95% conversion. Ceramic saddles (0.5 cm) preceded the catalyst to preheat the gas in the 2 × 40-cm-long quartz reactor tube. All tubing with SO_3 gas was heat traced at 150°C to avoid condensation. A Perkin-Elmer 257 infrared spectrometer with a 10-cm gas cell containing CaF_2 windows was used to evaluate the SO_2 concentration in the SO_3 scrubbed gas. Transmittance readings at 1170 cm^{-1} with air as a reference gave reactor exit SO_2 concentrations based on known inlet gas content. Conversions could then be calculated. A 30% converted gas could be supplied by varying the flow to the reactor and to the bypass around the reactor.

A Mettler TA-1 was used to perform differential thermal analyses (DTA), thermogravimetric analyses (TG), and derivative thermogravimetric analyses (DTG). About 250 mg of the catalyst sample to be analyzed was placed into a cylindrical alumina crucible that was 8 mm i.d. by 20 mm long. The reference crucible was the same except that it contained Al_2O_3 in a quantity that balanced the weight of the sample crucible. The crucibles were placed carefully upon Pt/Pt–10% Rh thermocouples which were contained in a sample holder. The sample holder rested on the Mettler balance and within the furnace so that the SO_2/SO_3 gas atmosphere would flow over the sample but not into the balance. Nitrogen or argon continually purged the Mettler balance for protection against the corrosive gas. Operating parameters were 30 scc/min SO_2/SO_3 feed gas, 160 scc/min argon, and a heating rate of 10°C/min.

The operating procedure used for running the Mettler consisted of weighing out the sample and reference and placing them onto the balance before enclosing the furnace. The balance was calibrated and the

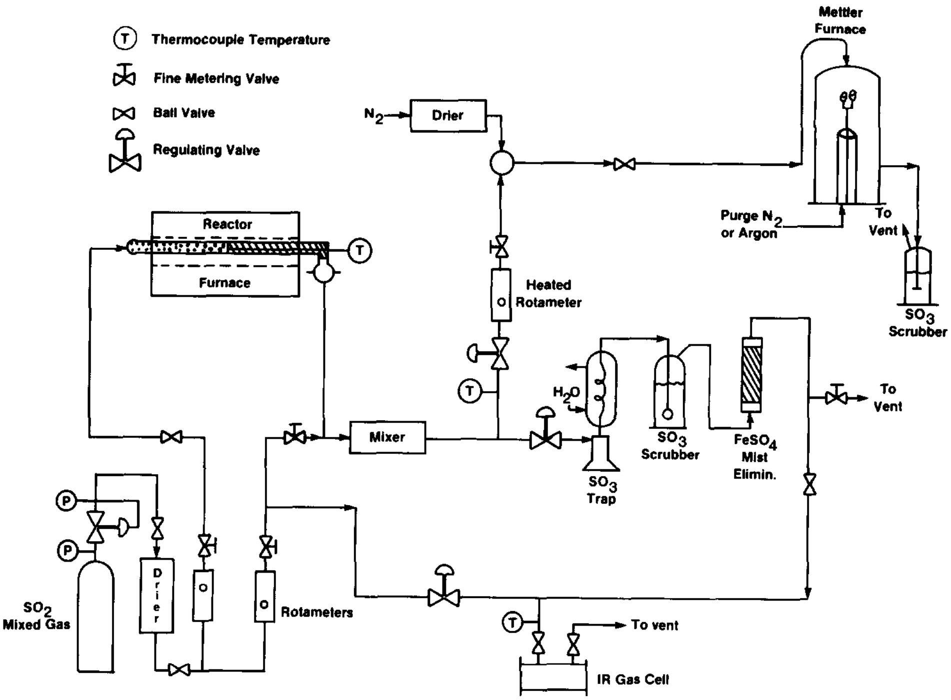

FIG. 1. SO_3 generator flow diagram.

system was then evacuated. When preparing for an SO_3 run, the 0.6-cm tubing between the Mettler and the SO_3 generator was purged with nitrogen overnight. The SO_3 generator was started up by opening the values for SO_2 flow through the reactor, turning on the heat tracers and the reactor furnace, and calibrating the IR gas analyzer with the SO_2 feed gas. 2 h were necessary to bring the reactor up to 480°C and to produce a steady SO_3 flow. In the meantime, the Mettler furnace was purged with argon after setting the flow with a bubble meter. The Mettler furnace was then brought up to 100°C and the heating cycle was begun after SO_3 gas was opened to the Mettler. Normally, three heating and cooling cycles were run before the scans became reproducible. The sample was left at the high temperature for 10 min and at 100°C for 20 min before cooling or heating.

Electron paramagnetic resonance (EPR) is a useful technique for detecting changes in concentration and state of V^{4+} ($3d'$) ions in vanadium catalysts. The EPR instrument used here was a Varian 4502 spectrometer which was equipped with a 22.5-cm magnet and Fieldial sweep system. The microwave bridge had been modified with addition of a Micronow low-power accessory. The modulation and synchronous detection system is shown in Fig. 2. The equipment consisted of a PAR HR-8 lock-in amplifier, a Krohn-Hite DCA-50 power amplifier, a Krohn-Hite MT-56 matching transformer, and a HP 3300A function generator. The reactor which was used for examining the catalyst samples under reaction conditions was a 0.3-cm-diameter quartz tube. The heating element consisted of two strips of platinum which had been applied as a paste (Engelhard No. 6082). The temperature was measured with a platinum/platinum–13% rhodium thermocouple. 50 mg of each catalyst (on 80–120-mesh CPG supports) were packed into the small quartz tube and

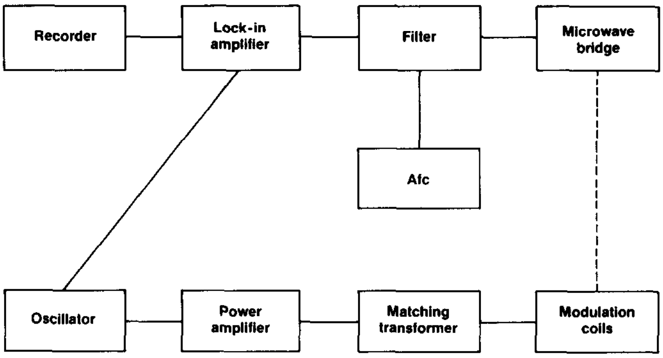

FIG. 2. EPR modulation and synchronous detection system.

about 50 scc/min of gas flowed through the catalyst. The resultant space velocity was 30,000 h^{-1} which gave differential conditions in the catalyst bed. The sample runs in SO_2–SO_3–O_2 atmospheres required the same operation of the SO_3 generator as for the Mettler experiments.

For most experiments, a modulation frequency of 32–34 kHz was applied. The modulation amplitude was always smaller than the linewidths of the signals observed. The maximum peak-to-peak modulation amplitude reaching the sample in the cavity was estimated to be 0.3 G. All the spectra were obtained as derivatives of the absorption signal at low-power levels with about 23 dB attentuation. At this low-power level, the variations of leakage current with changing temperature were not pronounced. A typical run used 30 or 95% preconverted (pc) 10% SO_2, 11% O_2 gas. The catalyst was allowed to come into equilibrium with the 95% pc gas at 500°C for several hours and with the 30% pc gas at 450°C overnight. The system was slowly cooled over a 2-day period down to 300°C in the gas being run. For each temperature below 400°C at which an EPR scan was taken, the sample was allowed to equilibrate with the gas for at least 4 h. Because there were three V^{4+} signals and each signal intensity was a function of temperature, catalyst vanadium concentration, and the SO_2/SO_3 gas concentrations, we could not reliably quantify the V^{4+} concentrations from the EPR data. EPR qualitative data was good enough for our reaction mechanism studies.

RESULTS

Mettler Thermal Analyses

As a control experiment, the CPG support was run in both 95 and 30% pc gas. On heat-up from 100 to 450°C, no thermal events appeared on the DTA scans, and no weight loss was seen. Thus, the CPG support was inert to the SO_2/SO_3 atmospheres. A $VOSO_4$–$5.7H_2O$ sample was heated in nitrogen at 700°C at 10°C/min. The sample showed very sharp endotherms on the DTA scan which peaked at 155 and 300°C. A 39% weight loss ending at 350°C with DTG minimums at 155 and 305°C corresponding to the endotherms was due to water desorption. A 27% weight loss began at 400°C and increased significantly at 500°C due to decomposition of $VOSO_4$ into V_2O_5 and SO_2 plus SO_3. A very large endotherm and DTG minimum due to this decomposition peaked at 645°C. V_2O_5 fused at 687°C.

A $K/V = 3$ low loading catalyst was run first in both 95 and 30% pc gases. Fig. 3 shows the results of a typical heat-up. The 95% pc gas gave a fairly large endotherm at 360°C on the DTA scan with a corresponding shoulder on the DTG scan. A second endotherm at 405°C matched the minimum on the DTG. This DTG minimum shows a maximum rate of weight loss at this temperature.

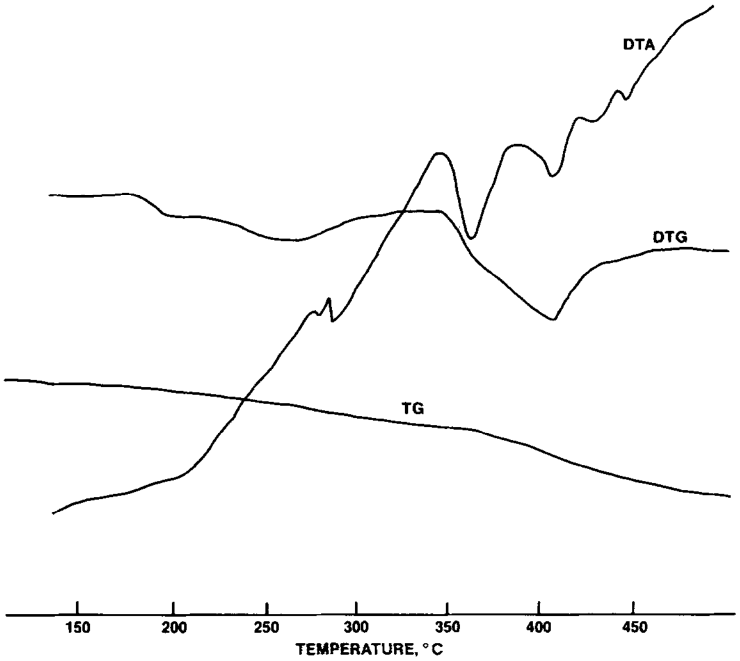

FIG. 3. K/V = 3, 0.027 g V/g support, 95% preconverted gas.

A high loading K/V = 3 catalyst was run on the Mettler to see what effect loading had upon the results. As can be seen in Fig. 4, the endotherms are larger but the total weight loss is not much different than that in Fig. 3. The DTG minimum at 425°C was much sharper than that seen for the low loading catalyst (Fig. 3). At the lower temperatures, there was an exotherm peaking at 290°C due to a solid state transition. Weight loss in both gases began at 340°C. As shown in Fig. 5, the 30% pc gas gave an even larger endotherm at 440°C than the 95% pc gas, but the DTG minimum at this temperature was not as sharp. The weight loss was 3% for the 30% pc gas and 5% for the 95% pc gas.

A high loading Cs/V = 3 catalyst was run to observe what effect cesium would have upon the results. For this catalyst in 95% pc gas, weight loss began at 250°C and only broad-ill-defined endotherms were observed between 300 and 400°C. The DTG hit a minimum at 365°C as shown in Fig. 6. A total weight loss of 6.5% occurred. This weight loss was 30% higher than the K/V catalyst. After cooling in argon from 475 to 100°C, the next heat-up showed a straight DTA scan and no SO_3 weight loss until 405°C. An inert gas apparently strips out SO_2/SO_3 so that any crystal formation does not occur.

The results for the Cs/V = 3 catalyst in 30% pc gas are given in Fig. 7. A 3.6% weight loss began at 320°C. A small endotherm occurred at 385°C and a larger endotherm peaked at 425°C corresponding to the DTG minimum at 435°C. It appears that the higher SO_2 and lower SO_3 gas concentrations cause all of the thermal events to occur at higher temperatures. To see what effect low oxygen in the gas would have upon the cesium catalyst, a 90% preconverted 10.5% SO_2, 5.38% O_2 gas was run over the catalyst. The results were very similar to those in Fig. 6 for the high O_2 gas. Oxygen does not affect the thermal analyses of the cesium catalyst. These results agree with those of Boreskov *et al.* (*8*) on EPR with potassium.

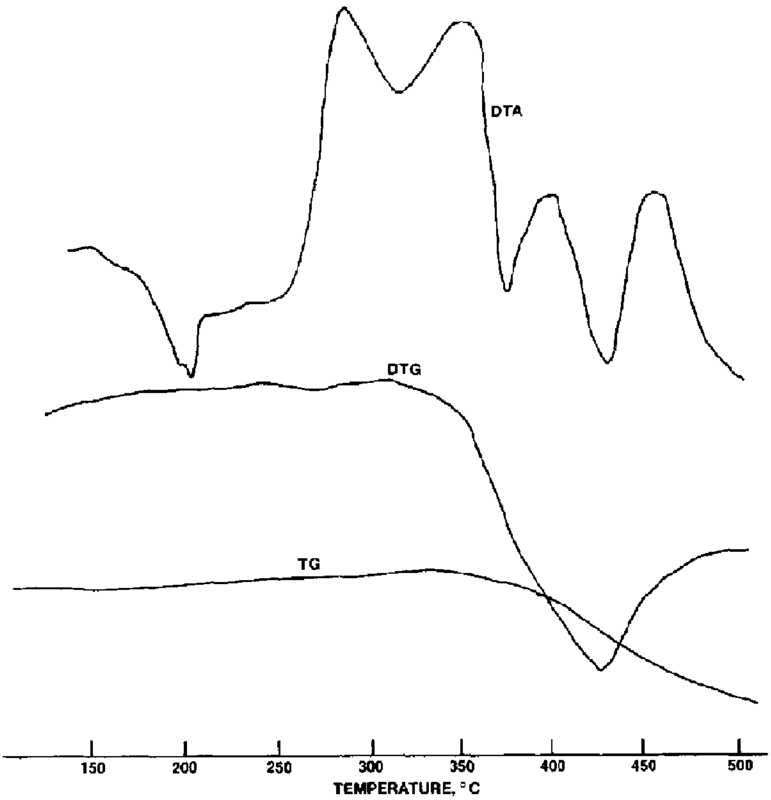

FIG. 4. K/V = 3, 0.08 g V/g support, 95% preconverted gas.

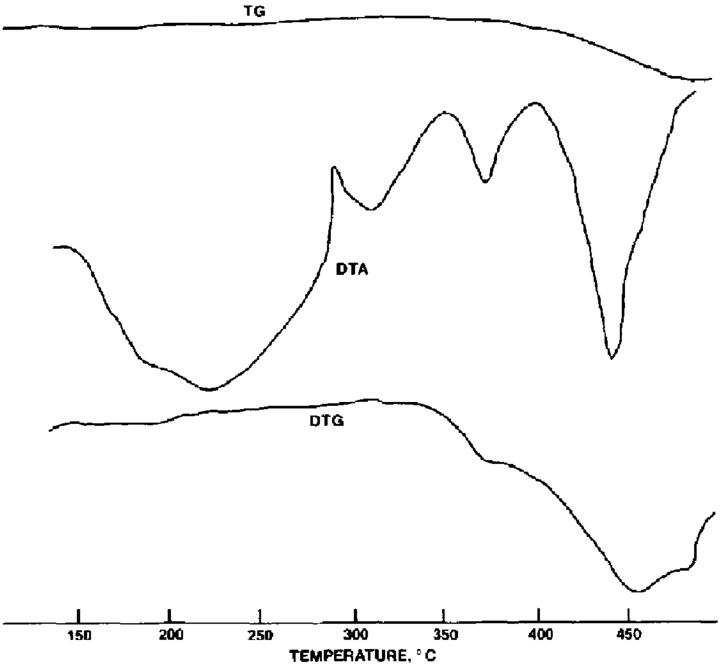

FIG. 5. K/V = 3, 0.08 g V/g support, 30% preconverted gas.

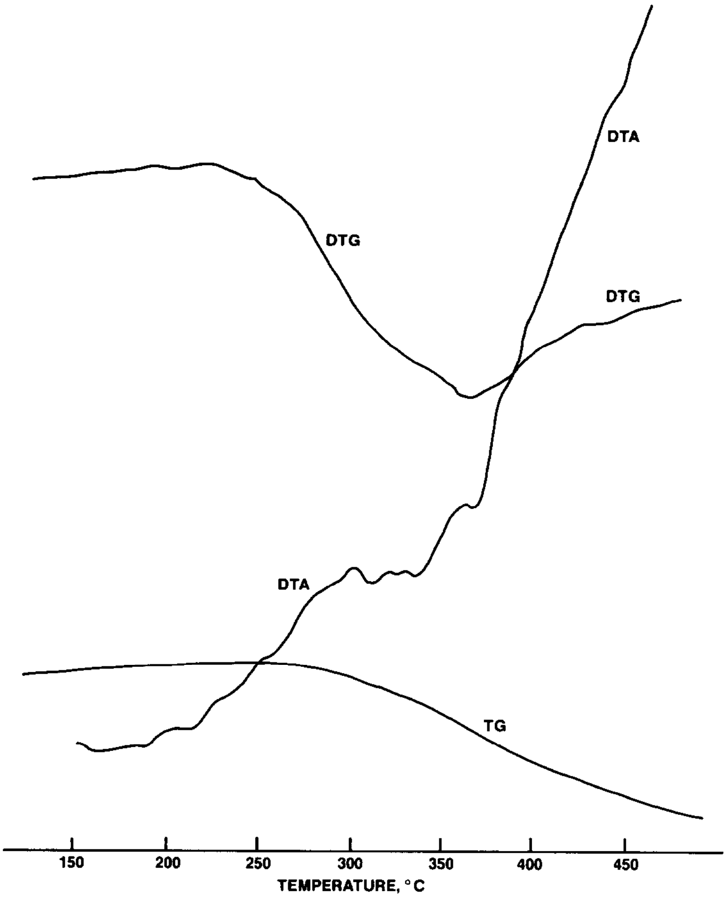

FIG. 6. Cs/V = 3, 0.08 g V/g support, 95% preconverted gas.

A lower loading Cs/V = 3.5 catalyst gave different results when compared to the Cs/V = 3 catalyst in 95% pc gas. Only small endotherms occurred at 370–390°C, weight loss began at 200°C, and the DTG minimum was at 300°C. Table I summarizes the Mettler results for the four catalysts.

EPR

The spectra that were obtained for the different samples could be divided into three different lineshapes: *A*, anisotropic hyperfine structure; *B*, isotropic hyperfine structure; *C*, single line. The anisotropic hyperfine structure of line *A* results from a low symmetry around the V^{4+} paramagnetic ions which are randomly oriented within the $K_2S_2O_7$–V_2O_5 salt. Spectrum *A* is usually referred to as a polycrystalline powder or glassy spectrum meaning that individual VO^{2+} sites are randomly oriented in

TABLE I

Mettler Results

Catalyst	% pc gas	Endotherm peak	DTG minimum	% Wt loss	Weight loss starting at
K/V = 3	95	405°C	405°C	5	350°C
0.027 g V/g support	30	410	410	2	330
K/V = 3	95	425	425	5	340
0.080 g V/g support	30	440	450	3	340
Cs/V = 3	95	365,390	365	6.5	250
0.080 g V/g suppor	30	425	435	3.6	320
Cs/V = 3.5	95	370,390	300	7	200
0.04 g V/g support	30	430	430	3	300

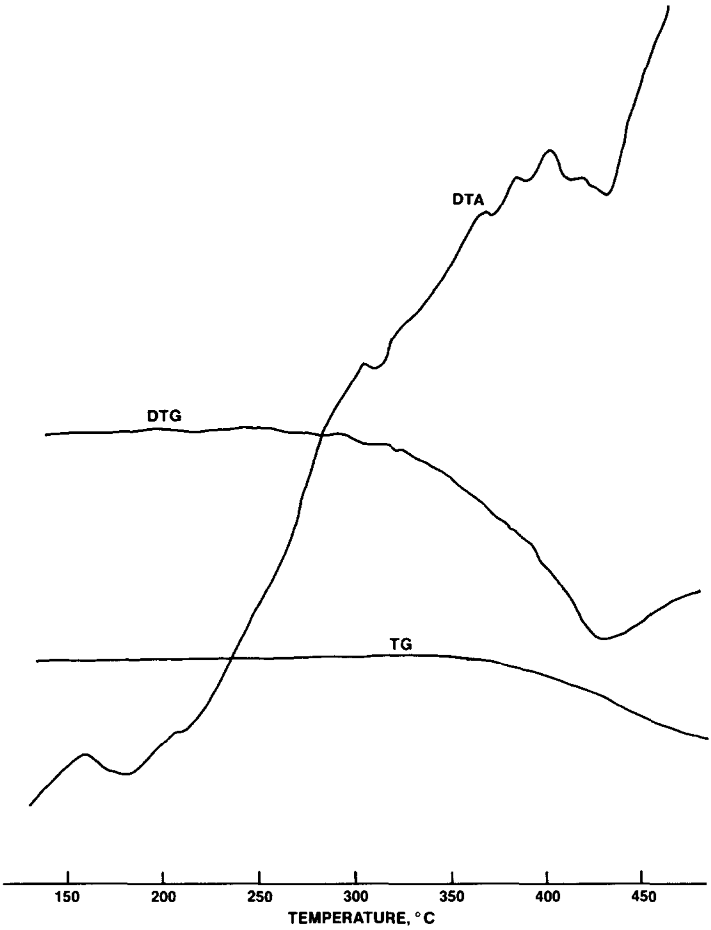

FIG. 7. Cs/V = 3, 0.08 g V/g support, 30% preconverted gas.

the solid state (*6, 7*). An isotropic hyperfine structure is important because the assymmetry of the lineshape is a measure of the viscosity of the solution. Therefore, line *B* is due to V^{4+} ions in solution (*7*). Single line *C* is exchange narrowed as a result of a sharp decrease in the mean distance between vanadium ions (*7*) and of the presence of a spin exchange interaction. A crystalline vanadium phase could cause the single line signal.

$VOSO_4$–$5.7H_2O$ was heated up in N_2 and the scans appear in Fig. 8. The instrument sensitivity at 116°C was only 40% of the sensitivity at the other temperatures. As can be seen, the signal for $VOSO_4$ is line *C*, and it becomes much weaker between 394 and 495°C. This weakening of the signal is due to $VOSO_4$ decomposition to V_2O_5, SO_3, and SO_2.

Results for a low loading K/V = 3 catalyst in 95% pc gas showed that a sharp signal (line *C*) first appeared at 401°C and slowly grew as temperature was decreased. In 30% pc gas a weak signal was present at 454°C after overnight exposure, and the signal became very strong at 380°C. More V^{4+} was present in the 30% pc gas than in the 95% pc gas. Upon heating in N_2, the sharp V^{4+} signal disappeared between 280 and 430°C. The higher loading K/V = 3 catalyst gave results similar to the low loading K/V catalyst, but the V^{4+} concentrations were much higher at each temperature.

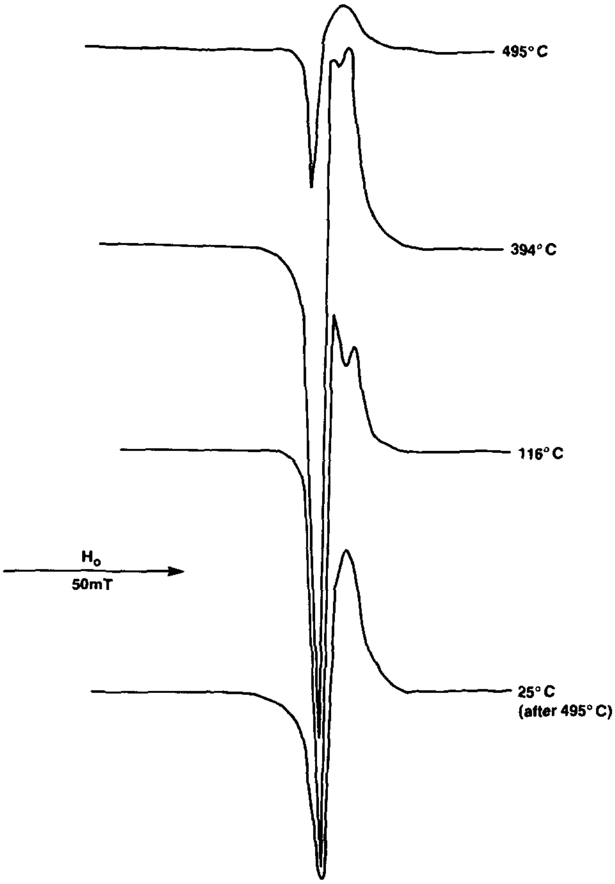

FIG. 8. EPR spectra for $VOSO_4 \cdot nH_2O$ in N_2.

The high loading Cs/V = 3 and K/V = 3 catalysts in 95% pc gas can be compared in Figs. 9 and 10. The only V^{4+} signals for the Cs/V = 3 catalyst were hyperfine lineshapes in Fig. 9. A spectrum of V^{4+} (or VO^{2+}) in a liquid phase (line *B*) first appeared at 401°C and increased in intensity with decreasing temperature, especially at 379°C. At 246°C the spectrum of V^{4+} in the solid state (line *A*) was observed. In the 30% pc gas, the same results were obtained except the sharp V^{4+} signal (line *C*) was visible at 340°C. After being in 30% pc gas overnight at 320°C, the catalyst was suddenly exposed to 95% pc gas and the sharp V^{4+} signal grew immediately. At 300°C the signal increased substantially. Apparently, the high amount of VO^{2+} present in the catalyst after exposure to high SO_2 flow picked up SO_3 and formed a V^{4+} crystal which precipitated out.

The spectra for the K/V = 3 catalyst appears in Fig. 10. At 452°C a symmetrical line was present. This line was probably due to V^{4+} polymers which were soluble in the thick films of the molten salt. At 423°C two signals appeared simultaneously and increased in intensity with decreasing temperature: one was hyperfine structure signifying V^{4+} ions in the solid state or solution, and the other was the exchange narrowed line *C*. In 30% pc gas line *C* was much larger at each temperature and grew significantly at 310°C. A high SO_2 gas concentration causes more V^{4+} crystal formation.

A lower loading Cs/V = 3.5 catalyst was

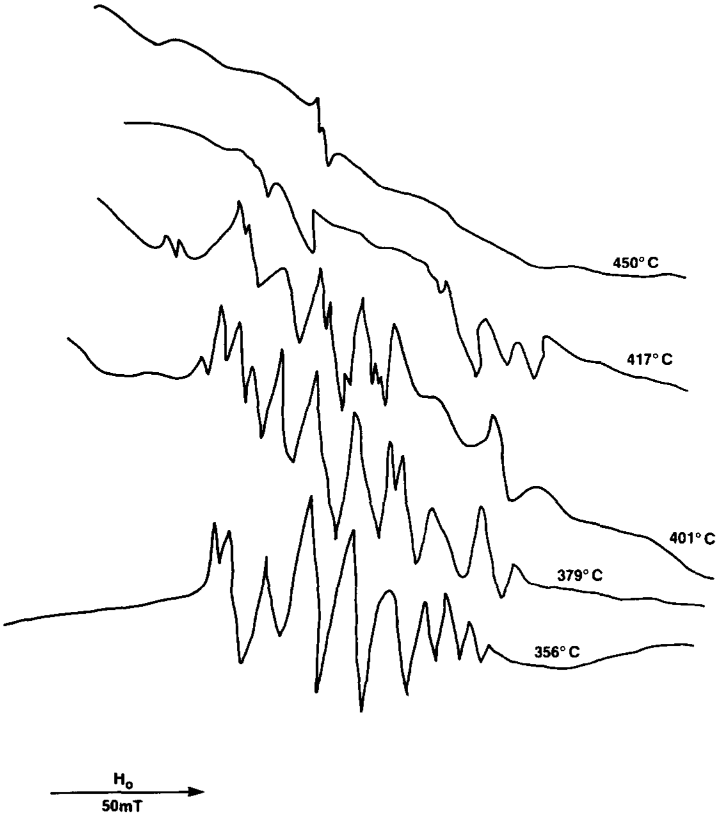

FIG. 9. Cs/V = 3, 0.08 g V/g support, 95% preconverted gas.

run in both gases and the results in Fig. 11 show the differences. Each gas was run through the catalyst from 450 to 300°C for 24 h before cooling and purging in N_2 at 150°C overnight. The 95% pc gas gave only line *A* which indicates VO^{2+} sites randomly oriented in the solid state. The 30% pc gas gave both line *A* and line *C*. These results indicate that higher SO_2 gas content is necessary to form large amounts of V^{4+} in the Cs/V = 3.5 molten salts before crystals precipitate out of the melt. As temperature was decreased from 450°C for the 95% pc gas, the hyperfine structure was evident at 400°C and grew as temperature was decreased. The molten salt was assumed to begin solidifying at 300°C because line A appeared. When unconverted 10% SO_2 gas was brought through at 300°C, line *C* grew within an hour. Apparently, the salt was still molten because SO_2 could diffuse into the melt to reduce V^{5+} and precipitate V^{4+}. In 30% pc gas much more V^{4+} was present on the catalyst and line *C* first appeared at 325°C and was very strong at 300°C. The catalyst had been kept at 350°C overnight in the 30% pc gas and line *C* did not appear. Thus, 24 h at 350°C still did not result in any V^{4+} precipitation within the Cs/V = 3.5 molten salt.

To summarize the EPR work on the catalysts, Table II shows which V^{4+} signals grew in at what temperatures while cooling down the reactor. It is apparent that the temperature at which appearance of V^{4+} occurred correlates well with the breaks on the Arrhenius plots of the potassium catalysts (*25*). The V^{4+} lines are very similar for the two potassium catalysts, but cesium gives different lines.

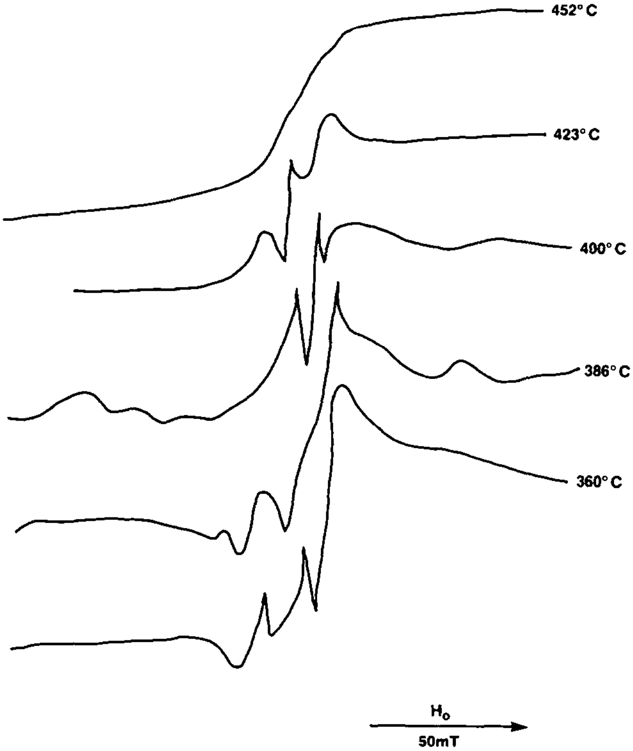

FIG. 10. K/V = 3, 0.08 g V/g support, 95% preconverted gas.

DISCUSSION

The results from the Mettler TA-1 and the EPR can be explained if we assume the following reactions at low temperature:

$$V_2O_4\text{–}SO_3 \text{ (solid)} \rightleftharpoons V_2O_4\text{–}SO_3 \text{ (liquid)} \quad (12)$$

$$V_2O_4\text{–}SO_3 \text{ (liquid)} \rightleftharpoons V_2O_5 + SO_2 \quad (13)$$

Reaction (12) is dissolution of the V^{4+} crystal into the molten salt and reaction (13) is the reverse of reactions (8) and (5). Reaction (8) is the intramolecular oxidation of the V_2O_5–SO_2 complex.

For the K/V catalysts, the first endotherm with weight loss at 360°C is believed to be due to melting of the molten salt. The second endotherm at 400–450°C with large weight loss agrees with the disappearance of the solid V^{4+} species on EPR. During heating we believe that the solid V^{4+} phase is dissolving and oxidizing according to reactions (12) and (13). Gas with little or large amounts of O_2 did not affect V^{4+} changes. Passing an inert gas through the catalyst at 400°C pushed reactions (12) and (13) to the right and removed the thermal events on

TABLE II

Summary of EPR Results

Catalyst	% pc gas	T_B	$T_{V^{4+}}$	EPR lines		
				A	*B*	*C*
K/V = 3	95	412°C	401°C			+ +
0.027 g V/g support	30		425			+ +
K/V = 3	95	425	423	+	+	+ +
0.08 g V/g support	30		450			+ +
Cs/V = 3	95	400	401	+	+ +	
0.08 g V/g support	30		422	+	+ +	+ (340°C)
Cs/V = 3.5	95	390	400	+	+ +	
0.04 g V/g support	30		450	+	+ +	+ (325°C)

Note. T_B, Temperature at break on the Arrhenius plot (25); $T_{V^{4+}}$, temperature at which designated V^{4+} signal first grew in; +, V^{4+} signal that was present; + +, the V^{4+} signal that grew in at $T_{V^{4+}}$; *A*, V^{4+} ions in solid state; *B*, V^{4+} ions in solution; *C*, V^{4+} crystallite complex.

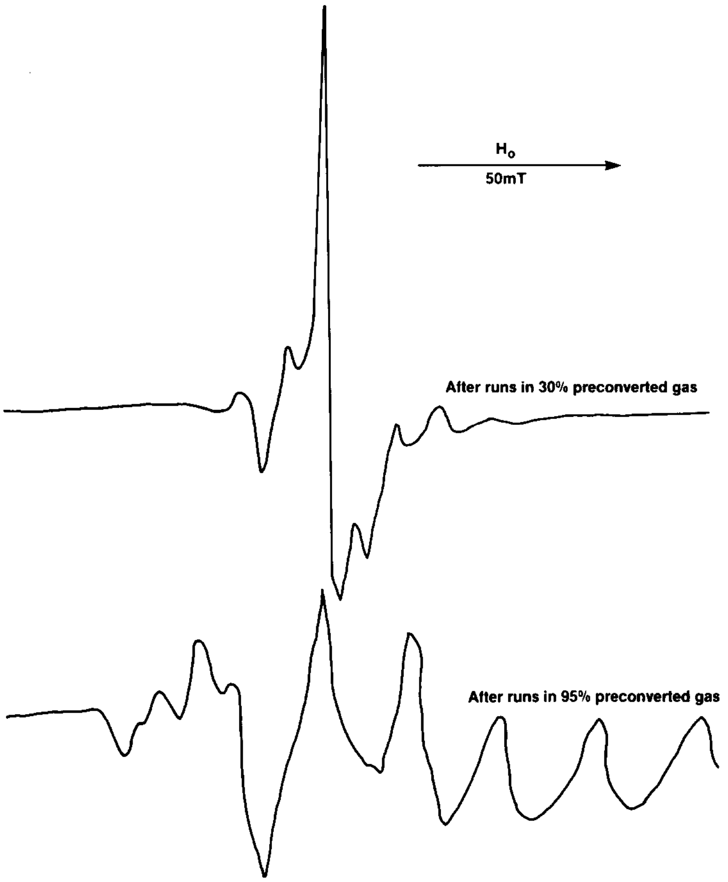

FIG. 11. Cs/V = 3.5, 0.04 g V/g support, T = 150°C.

the Mettler and V^{4+} on the EPR. Using 30% pc gas increased SO_2 gas concentration which pushed reactions (13) and (12) to the left. Larger thermal events and more V^{4+} on the EPR resulted. Table III shows excellent agreement between the analytical results and the breaks on the Arrhenius plots for the K/V catalysts. Thus, the K/V catalysts lose significant activity below 425°C because a V_2O_4–SO_3 compound precipitates from the molten salt.

The analytical results of the cesium catalysts were different from the potassium catalysts. The thermal analyses showed SO_3 weight loss beginning at much lower temperatures (below 300°C), broad ill-defined endotherms above 300°C and DTG minimums at lower temperatures. 30% pc gas

TABLE III

Summary of Analytical Results

Catalyst	T_B	Temperature of mettler peaks	$T_{V^{4+}}$
K/V = 3 0.027 g V/g support	405°C	405°C	401°C
K/V = 3 0.08 g V/g support	425	425	423
Cs/V = 3 0.08 g V/g support	400	365,390	401
Cs/V = 3.5 0.04 g V/g support	390	370,390	400

Note. $T_{V^{4+}}$ is the temperature at which line C first appeared on EPR for the K/V catalysts and line B first appeared on EPR for the Cs/V catalysts. Mettler peak temperature is the average of the DTG minimum and the upper endotherm peak. T_B is the temperature at which the break on the Arrhenius plot occurred (*25*).

did increase the thermal events and made them occur at higher temperatures when compared to 95% pc gas. EPR only showed V^{4+} ions in solution down to 300°C for 95% pc gas. 30% pc gas showed more V^{4+} than 95% pc gas. The Cs/V = 3 catalyst showed more V^{4+} than the Cs/V = 3.5 catalyst.

Our results suggest the following differences between the cesium and potassium catalysts:

(1) The cesium catalyst has a greater affinity for SO_3. The higher Cs/V ratio increases this SO_3 affinity.

(2) The large cesium cation could be withdrawing SO_3 from the V^{4+} complex which would prevent precipitation of the V_2O_4–SO_3 in reaction (12).

(3) The strong dependence of the V^{4+} content on the SO_2/SO_3 gas concentrations indicates that reactions (12) and (13) can also occur for the cesium catalysts.

The unexpected result is that the kinetics for the cesium catalysts (*25*) showed sharp breaks on the Arrhenius plots at 400°C. Table III shows that dissolved V^{4+} in the Cs/V catalysts did appear on the EPR at 400°C and increased as temperature was decreased.

The Cs/V results can be explained in the following way:

(a) As temperature drops to 400°C, the equilibrium for reaction (8) moves to the right and V_2O_4–SO_3 forms (see Refs. (*18, 20*)).

(b) Increasing SO_2 with 30% pc gas will move the equilibrium of reactions (5) and (8) to the right. More V_2O_4–SO_3 forms and reaction (12) will move left to precipitate V_2O_4–SO_3 (see Ref. (*5*)).

(c) Increasing SO_3 after running in high SO_2 gas at 320°C will move reactions (9) and (12) left to precipitate V_2O_4–SO_3.

(d) The overall oxidation of SO_2 will slow down at 400°C because more V_2O_4–SO_3 will form according to reaction (8). Since the high SO_3 content in 90+% converted gas mixtures will keep equilibrium reaction (9) to the left, reaction (10) will slow. Less V_2O_5 will then be available for the associative mechanism which included reactions (5) to (7) (see Ref. (*20*)). Simonova *et al.* (*26*) replaced portions of potassium with sodium and also saw increases in catalyst activity and decreases in V^{4+} precipitation. The explanation in (a)–(d) above for the cesium catalysts can also be applied to the sodium results.

CONCLUSIONS

(1) Our work with Mettler thermal analysis and EPR spectroscopy confirms that V^{4+} precipitation at temperatures below 450°C causes the sharp loss in K/V catalyst activity and the activation energy increase at the lower temperatures.

(2) The Cs/V catalysts increase the solubility of the V^{4+} compounds below 400°C, but the catalyst activation energy still increases at 400°C.

(3) The six-step reaction mechanism of Boreskov *et al.* (*18, 20*) does explain why the Cs/V catalysts lose activity quickly below 400°C even though V^{4+} compounds do not precipitate from the melt.

REFERENCES

1. Urbanek, A., and Trela, M., *Catal. Rev.-Sci. Eng.* **21,** 73 (1980).

2. Villadsen, J., and Livbjerg, H., *Catal. Rev.-Sci. Eng.*, **17,** 203 (1978).

3. Donovan, J. R., Stolk, R. D., and Unland, M. L., *in* "Applied Industrial Catalysis" (B. E. Leach, Ed.), Vol. 2, p. 245. Academic Press, New York, 1983.

4. Kenney, C. N., *Catal. London* **3,** 123 (1980).

5. Grydgaard, P., Jensen-Holm, H., Livbjerg, H., and Villadsen, J., *ACS Symp. Ser.* **65,** 582 (1978).

6. Boreskov, G. K., Davydova, L. P., Mastikhin, V. M., and Polyakova, G. M., *Dokl. Akad. Nauk* **171,** 648 (1966).

7. Mastikhin, V. M., Polyakova, G. M., Zyulkovskii, Y., and Boreskov, G. K., *Kinet. Katal.* **11,** 1463 (1970).

8. Boreskov, G. K., Polyakova, G. M., Ivanov, A. A., and Mastikhin, V. M., *Dokl. Akad. Nauk* **210,** 626 (1973).

9. Mars, P., and Maessen, J. G., *J. Catal.* **10,** 1 (1968).

10. Ponomarev, V. E., Ketov, A. N., Balzhinimaev, B. S., Ivanov, A. A., and Kozyrev, S. V., *React. Kinet. Catal. Lett.* **18,** 421 (1981).

11. Holroyd, F. P. B., Ph.D. Thesis, Cambridge University, 1968.
12. Holroyd, F. P. B., and Kenney, C. N., *Chem. Eng. Sci.* **26,** 1963, 1971 (1971).
13. Ezhkova, Z. I., Zaitsev, B. E., Konysheva, L. I., *et al., Kinet. Katal.* **13,** 1288 (1972).
14. Hahle, S., and Meisel, A., *Kinet. Katal.* **12,** 1276 (1971).
15. Wolf, F., Kruger, W., and H. Furtig, *Chem. Technol.* **24,** 753 (1972).
16. Guo, H., Han, Z., and Xie, K., *Huagong Xuebao (Taiwan)* **2,** 139 (1984).
17. Boreskov, G. K., Ivanov, A. A., Balzhinimaev, B. S., and Karnatovskaya, L. M., *React. Kinet. Catal. Lett.* **14,** 25 (1980).
18. Kozyrev, S. V., Balzhinimaev, B. S., Boreskov, G. K., Ivanov, A. A., and Mastikhin, V. M., *React. Kinet. Catal. Lett.* **20,** 53 (1982).
19. Chumachenko, V. A., Balzhinimaev, B. S., Karnatovskaya, L. M., Matros, Yu. Sh., and Oruzheinikov, A. I., *React. Kinet. Catal. Lett.* **20,** 145 (1982).
20. Balzhinimaev, B. S., Ponomarev, V. E., Boreskov, G. K., and Ivanov, A. A., *React. Kinet. Catal. Lett.* **25,** 219 (1984).
21. Balzhinimaev, B. S., Ponomarev, V. E., Boreskov, G. K., Ivanov, A. A., Sheplev, V. S., and Sadovskaya, E. M., *React. Kinet. Catal. Lett.* **28,** 81 (1985).
22. Hansen, N. H., Fehrmann, R., and Bjerrum, N. J., *Inorg. Chem.* **21,** 744 (1982).
23. Krasil'nikov, V. N., Glazyrin, M. P., and Ivakin, A. A., *Neorg. Khim.* **28,** 2111 (1983).
24. Mastikhin, V. M., Lapina, O. B., and Simonova, L. G., *React. Kinet. Catal. Lett.* **26,** 431 (1984).
25. Doering, F. J., and Berkel, D. A., *J. Catal.* **103,** 126 (1987).
26. Simonova, L. G., Lapina, O. B., Mastikhin, V. M., and Dzisko, V. A., *React. Kinet. Catal. Lett.* **22,** 59 (1983).